1995

Static Pressure at the Ground Under Atmospheric Flow Across a Windbreak

James R. Brandle
University of Nebraska - Lincoln, jbrandle1@unl.edu

Published in the preprint volume of the **11TH SYMPOSIUM ON BOUNDARY LAYERS AND TURBULENCE**, March 27-31, 1995, Charlotte, NC, by the American Meteorological Society, Boston, MA.

P14.48

STATIC PRESSURE AT THE GROUND UNDER ATMOSPHERIC FLOW ACROSS A WINDBREAK

R.A. Schmidt*, E.S. Takle, J.R. Brandle, and I.V. Litvina

USDA Forest Service, Laramie, Wyoming
Iowa State University, Ames, Iowa
University of Nebraska, Lincoln, Nebraska
Agrophysical Research Institute, St. Petersburg, Russia

1. INTRODUCTION

Many studies of windbreak aerodynamics have focused on the two-dimensional model of flow perpendicular to a windbreak, in conditions of neutral stability. Extending these models to oblique winds with a diurnal pattern of thermal stratification requires still more work to understand how windbreak architecture determines turbulent structure in sheltered areas. Both average gradients and fluctuation of static pressure are pieces of information critical to this extension.

The objective of this paper is to describe our initial efforts to measure average static pressures at the surface during field studies of wind reduction by shelterbelts. Our intentions are to (1) estimate windbreak pressure-loss coefficients, and (2) evaluate pressure-gradients as forces that effect flow near and through the windbreak.

Optical porosity is the parameter most used to relate wind reduction to windbreak structure (see reviews by Heisler and DeWalle, 1988; Taylor, 1988). For thin barriers such as fences, porosity is an easily determined predictor of aerodynamic drag. However, for tree-rows (shelterbelts) and other vegetative windbreaks, relationships between porosity and drag are less clear.

An alternative used to relate windbreak structure to aerodynamic drag is a pressure-loss coefficient, determined by the drop in static pressure at the surface, between points immediately upwind and downwind of the barrier. This pressure drop Δp is usually normalized by the dynamic pressure of the approach flow, to define a resistance coefficient, $k_r = \Delta p/(\frac{1}{2}\rho u^2)$. The associated reference approach velocity is u, and ρ denotes fluid density. In wind-tunnel experiments (e.g. Plate, 1971), static pressure at the wall is often expressed in terms of a pressure coefficient $C_p = \Delta p/(\frac{1}{2}\rho u^2)$, where $\Delta p = (p - p_\infty)$ is the difference between local static wall pressure, p, and some reference, p_∞. The resistance coefficient is the difference between wall pressure coefficients upwind and downwind of the barrier.

Heisler and DeWalle (1988, Fig. 1) summarized wind tunnel measurements of resistance coefficients for screens. In addition to screen porosity, k_r depended on screen element shape. By the usual definition given above, Wilson's (1985, p. 133) measurements on a 50% porous fence in a wind tunnel gave k_r very close to 1.0. McNaughton (1988, p. 20) noted that resistance coefficient had not been measured in field studies. However, this is not a shortcoming of more recent studies (e. g., Litvina and Takle, 1993).

2. METHODS

In addition to details of the pressure measurements, this section briefly describes the wind profiling apparatus, and shelterbelt structure. Schmidt et al. (1995) provide more details of the data acquisition system, windbreaks, and procedures. The study site was the University of Nebraska research farm approximately 50 km north of Lincoln, Nebraska, USA (Section 26, 41°09′ N, 96°30′ W, 343 m elevation). Shelterbelt arrays on the farm provide several combinations of species and heights.

2.1 Pressure System

Wind tunnel studies (Plate, 1971, Fig. 9) provided an estimate of the expected range in differential pressure. For a 10 m/s reference wind speed, a pressure coefficient of -0.5 would require a sensor range of 25 Pa (25 N/m^2, or 250 μb, approximately 0.1 inch water). The selected sensor (Setra Systems* model 264) required only 6 mA at 12 V dc, making it suitable for battery operation. Adding a 2:1 voltage divider reduced the output voltage (0-5 V dc) for recording by

*Corresponding author address: R. A. Schmidt, USDA Forest Service, Rocky Mountain Forest and Range Experiment Station, 222 S. 22nd Street, Laramie, WY, USA. Phone (307) 742-6621 Fax (307) 742-0397

*The use of trade and company names is for the benefit of the reader; such use does not constitute an official endorsement or approval of any service or product by the authors institutions, to the exclusion of others that may be suitable.

data loggers (Campbell Scientific* model CR10). Specified sensor accuracy (0.4% of full scale, option 708) was 0.1 Pa (1 μb). Temperature effects on sensor zero and span varied between sensors. We found a maximum -3.3 μb/°C drift in zero over a field temperature range of 10 to 40°C. This was slightly larger than the specified ±3.3%FS/55°C for zero and span combined. The time constant given by the manufacturer was 50 ms, without filters on the input ports.

Automotive vacuum tubing (5/16 in nominal, 8 mm O.D., 4 mm I.D.) extended from sensor ports to points of measurement, over distances as far as 80 m. A single layer of 50-μm-mesh filter fabric protected open tube ends from foreign particles. We laid the tubing on the soil with the end pointed downwind, usually beneath a crop canopy. No other special termination was used.

Initial tests in September, 1993, with one sensor, measured the pressure drop across a two-row, ash-conifer shelterbelt, 12 m high. Three pressure sensors provided measurements around a 4.8-m, two-row redcedar windbreak in May, 1994. A 12-port scanning valve (Scanivalve Corp.* model KEM/1P-12T) switched between tubes from locations near a riparian strip and an ash-conifer belt, in July, 1994 (Fig. 1). Settling time between switching and sampling was 5 s, to account for filtering by the long tubes.

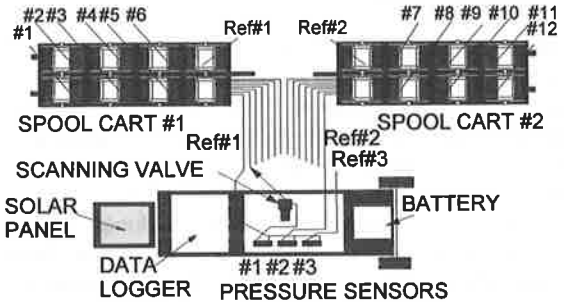

FIG. 1. The system for field measurements of static pressure evolved (by July, 1994) to include a hand cart with the data logger, pressure sensors, and 12-port scanning valve. Two carts carried spools of tubing. The diagram shows the interconnections. All ports have equal tube lengths (110 m), except Ref#3.

2.2 Wind and Temperature Profiles

Three portable 10-m masts (Jairell et al., 1984) supported temperature and wind speed sensors at ten levels. Temperature sensors were thermistor networks (YSI* 44203), in radiation shields. Cup anemometers (Maximum Inc.* model 40) were of high-impact plastic with low inertia. A data logger on a hand cart at each mast accumulated 5-min averages of the vertical profiles, wind direction from a propeller-vane, radiation, and relative humidity at 1.5-m height. Data loggers at the three masts and the pressure system were synchronized through radio links to a computer in a mobile van (Schmidt et al., 1995).

During measurements, we left one mast at a distant upwind location and moved the other two to positions upwind and lee of the windbreak. Wheels on the mast bases facilitated relocation within a 5-min interval. At least three 5-min runs at each location provided sets for averaging.

2.3 Shelterbelt Structure

The ash-conifer shelterbelt, planted in 1966, has two rows, 5 m apart. In each row, spacing is 2.5 m, with alternate species in pairs, two ash, two conifer, etc. Between rows, ash are opposite conifers. The ash (*Fraxinus pennsylvanica*) provide the average maximum 12-m height. Conifers, mostly eastern redcedar (*Juniperus virginiana* L.), with some Austrian pine (*Pinus nigra* Arnold), were shorter, increasing foliage in the lower part of the belt. Average base width to outside branch tips is 10 m. Ash leaf-fall was nearly complete at the time pressure measurements began. Schmidt et al. (1995) estimated optical porosity from night photographs of the shelterbelt back-lit by electronic flash.

The two rows of the eastern redcedar windbreak are 2.5 m apart, with trees at 2.5-m spacing. Planted in 1986, average maximum tree height was 4.75 m at the time of our measurements. Trees in the downwind row are between locations of trees in the upwind row. Distance across the shelterbelt between branch tips at the base was 6.2 m. Most of our measurements were with southerly winds over alfalfa 25 to 35 cm high. In the lee, freshly planted, 10-cm furrows ran perpendicular to the belt.

A wooded riparian strip transects the farm, providing a barrier with 7.3 m average maximum height near our measurement transect. (To measure heights, a distant observer with binoculars reads a survey rod at the belt.) Species include plum (*Prunus americana*), chokecherry (*Prunus virginiana*), willow (*Salix nigra*), and Siberian elm (*Ulmus pumila* L.). Cleared in 1986, most of the taller trees root in the upper banks, forming a cavity in the foliage, directly above the waterway. We made no estimate of optical porosity of this strip, which is 25-30 m wide. At the time of

pressure measurements, 15-cm wheat stubble covered the fetch, and 2-m corn adjoined the lee edge.

3. RESULTS

Because these were initial investigations with equipment new to us, configurations and objectives changed for each of the three measurement periods. Results are presented by field period, to show this progression.

3.1 September, 1993: 12-m ash-conifer

These tests showed that the selected sensor was of suitable range and stability for field measurements. During an 8-hour period on 28 September (Fig. 2), northwest wind averaged 321°, with 9.4° standard deviation. Five-min average static pressure loss across the east-west shelterbelt (Fig. 2a) ranged as high as 130 μb in a run with 6.5 m s^{-1} mean 10-m wind speed. The reference wind speed was from a mast 92 m south of the shelterbelt, because the approach was complicated by upwind barriers for northwest flow. Tube ends were 12 m upwind of the windward row (centerline), and 7 m downwind of the lee row, making the distance between pressure ports 24 m. The maximum 5-min pressure drop produced a gradient of 5.4 μb m^{-1}, equivalent to 5.4 mb km^{-1}.

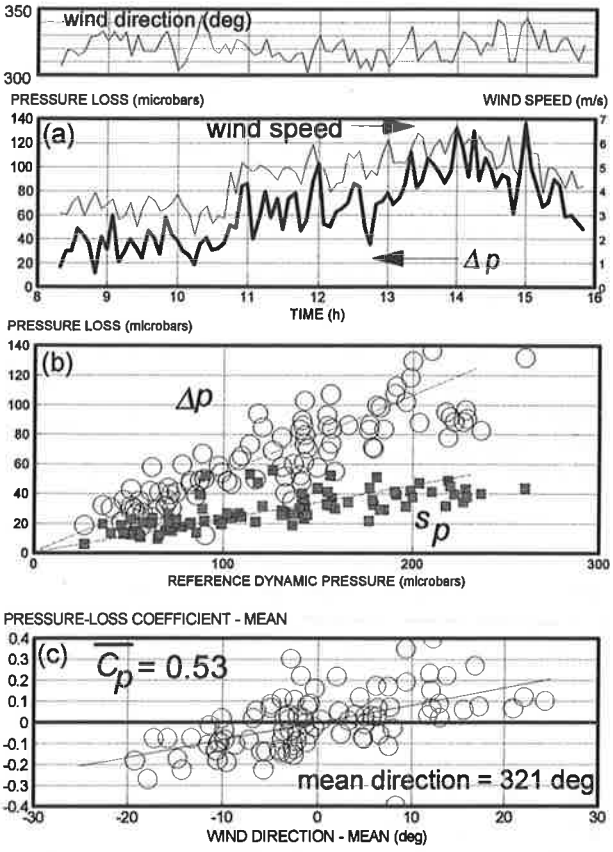

FIG. 2. Pressure differences (a) measured with oblique flow (39°) across a 12-m ash-conifer windbreak in September, 1993, gave us our first look at (b) range, variance, and (c) wind angle effects. For 91 runs (temperatures 13-22°C), pressure-loss coefficient averaged 0.53. See text for more details.

Sampling at 5-s intervals provided measures of the standard deviation of the pressure, s_p. The variation of s_p with reference dynamic pressure (Fig. 2b) is substantially larger than the variation associated with wind speed. Mean pressure-loss coefficient for the 91 five-minute averages was 0.53, with a standard deviation of 0.138. Average pressure loss decreased by 1 microbar per degree of wind angle deviation from perpendicular (360°). Extrapolating a regression of pressure-loss coefficient on wind angle (Fig. 2c) gave an estimated 0.84 for the pressure-loss coefficient in a perpendicular wind.

3.2 May, 1994: 4.8-m redcedar

With two additional sensors, we explored the distribution of static pressure at the surface over greater distances upwind and downwind of the barrier (Fig. 3a). Distribution of pressure coefficient C_p showed the expected increase, loss, and recovery for both southwest (SW), and south (S) flow over the redcedar belt on 10 and 13 May, respectively. Circles denote averages of three or more 5-min runs. Squares mark the average of all runs at that location. Attempts to use a scanning valve showed the need for modifications to improve field operations.

3.3 July, 1994: 7.3-m riparian and 12 m ash-conifer

With a battery-driven scanning valve, and spool carts to manage the tubing, we measured distributions of static surface pressure through both barriers. The pressure coefficient changed sign near the center of the barrier (Fig 3b and c). Each plot shows means and standard deviations during approximately 1 h (n = runs) when wind direction was steady. Each 5-min run-average is for 5 measurements. The wind angle shown on each plot is the deviation from perpendicular (north for the ash-conifer, west for the riparian). Both pressure loss and standard deviation for the ash-conifer (Fig. 3b) show the effect of the upwind belt.

3.4 Summary of Results

Surface static pressure is maximum at the upwind barrier face and shows a uniform decline to a minimum at the downwind face. Variance is greater downwind of the barrier, minimum at the windward face. Pressure loss decreases as attack angle increases from perpendicular. Pressure gradients across shelterbelts are as large as mesoscale gradients associated with severe winds.

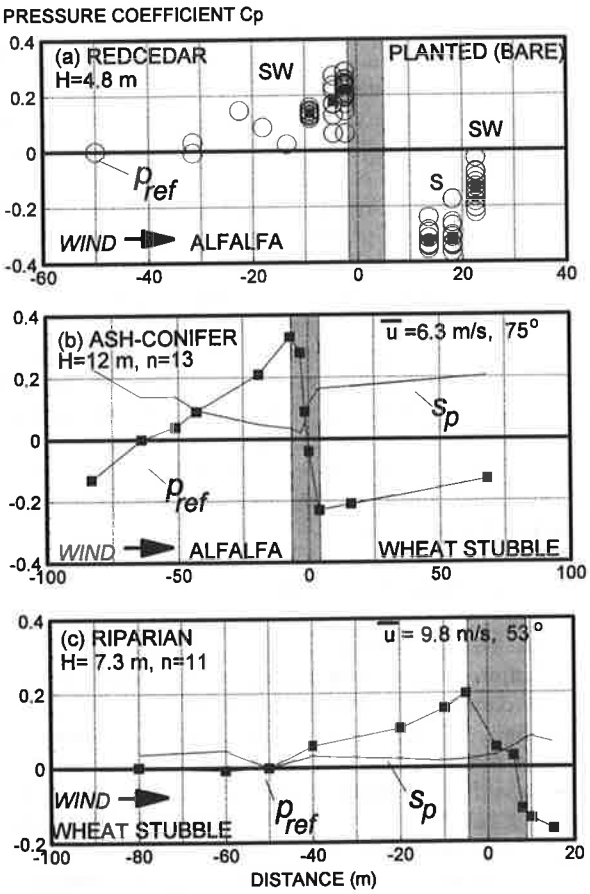

FIG. 3. For three barriers in oblique winds, average values of static pressure coefficient at the ground show the expected windward increase, loss through the belt, and downwind recovery. Average maximum barrier height is H. Shaded bands show the width of the barrier, and p_{ref} marks the location of the reference pressure. In (b) and (c), the number of runs averaged is n, standard deviation is marked s_p, and mean 10-m reference speed, u. Attack angle is measured from perpendicular, in degrees.

4. DISCUSSION

Resistance coefficients of screens (Heisler and DeWalle, 1988, Fig. 1) decrease as optical porosity increases. Applied to shelterbelts, wind at oblique attack angles should encounter a less-porous barrier, thus increasing pressure loss. Our measurements show the opposite. Part of the reason may be flow response to the pressure gradients.

Forces created by gradients of static pressure act perpendicular to a windbreak. Flow decelerates in the positive gradient on the windward side. The pressure drop accelerates wind through the shelter, and the recovery gradient decelerates air in the lee. With oblique wind, the pressure gradient also forces deflection, increasing the attack angle of approach flow. As air reaches the windward face, the sharp change to a favorable gradient turns flow toward (through) the barrier. In the lee, the recovering pressure again causes deflection toward the oblique approach angle. This pattern is clear in the flow-visualization photographs of Mulhearn and Bradley (1977). A companion paper to ours (Wang and Takle, 1995) considers these forces in more detail.

6. REFERENCES

Heisler, G. M., and D. R. DeWalle, 1988: Effects of windbreak structure on wind flow. *Agric. Ecosystems Environ.*, 22/23, 41-69.

Jairell, R. L., R. D. Tabler, and R. A. Schmidt, 1984: Portable ten-meter instrument mast. *Proceedings, Western Snow Conference,* April, 1984, Sun Valley, ID. Colorado State University, 168-171.

Litvina, I. A., and E. S. Takle, 1993: Snow deposition by shelterbelts as a means of reducing fire potential. 12th International Conference on Fire and Forest Meteorol. Jekyll Is. GA. 749-756.

McNaughton, K. G., 1988: Effects of windbreaks on turbulent transport and microclimate. *Agric. Ecosystems Environ.*, 22/23, 17-39.

Mulhearn, P. J., and E. F. Bradley, 1977: Secondary flows in the lee of porous shelterbelts. *Boundary-Layer Meteor.* 12, 75-92.

Plate, E., 1971: The aerodynamics of shelterbelts. *Agric. Meteorol.* 8, 203-222.

Schmidt, R.A., R. L. Jairell, J. R. Brandle, E. S. Takle, and I. V. Litvina, 1995: Windbreak shelter as a function of wind direction. *Proc. 9th Symposium on Meteorological Observations and Instrumentation*, 27-31 March, Charlotte, NC. Amer. Meteor. Soc., Boston, MA.

Taylor, Peter A., 1988: Turbulent wakes in the atmospheric boundary layer. *In*: Steffen, W. L. and O. T. Denmead (eds.) *Flow and Transport in the Natural Environment: Advances and Applications*, Proc. of an Int. Symp., Canberra, 1987. Springer-Verlag, New York, 270-292.

Wang, H. and E. S. Takle, 1995: Simulations of mean and turbulent properties of oblique flows near agricultural shelterbelts. *Proc. 11th Symposium on Boundary Layers and Turbulence*, 27-31 March, Charlotte, NC. Amer. Meteor. Soc., Boston, MA. (this volume).

Wilson, J. D., 1985: Numerical studies of flow through a windbreak. *J. Wind Eng. and Industr. Aerodyn.*, 21:119-154.